SPANDIDOS PUBLICATIONS

ONCOLOGY LETTERS 18: 2322-2329, 2019

Hepatocellular carcinoma grading and recurrence prediction using T_1 mapping on gadolinium-ethoxybenzyl diethylenetriamine pentaacetic acid-enhanced magnetic resonance imaging

XIALI QIN[1*], TENGFEI YANG[1*], ZHONGKUI HUANG[1], LILING LONG[1], ZHIPENG ZHOU[1], WENMEI LI[1], YINJUAN GAO[1], MENGZHU WANG[2] and XIAOYONG ZHANG[2]

[1]Department of Radiology, The First Affiliated Hospital of Guangxi Medical University, Nanning, Guangxi 530021; [2]Department of Magnetic Resonance Scientific Marketing, Siemens Healthineers, Guangzhou, Guangdong 510620, P.R. China

Received December 7, 2018; Accepted May 23, 2019

DOI: 10.3892/ol.2019.10557

Abstract. The aim of the present study was to explore the value of T_1 mapping on gadolinium-ethoxybenzyl diethylenetriamine pentaacetic (Gd-EOB-DTPA)-enhanced magnetic resonance imaging (MRI) for grading hepatocellular carcinoma (HCC) and predicting its recurrence rate. A retrospective study was performed that included 75 patients (66 men and 9 women; mean age, 52.89 years; age range, 23-79 years) with HCC who had undergone Gd-EOB-DTPA-enhanced MRI with T_1 mapping before surgery. The T_1 relaxation time of the 81 lesions and non-tumorous liver parenchyma in 75 patients with HCC were measured before Gd-EOB-DTPA was injected and then at 5, 10 and 20 min after administration, respectively. $T_{1[\text{lesion (L)-hepatic parenchyma (H)}]/H}$ (%) was calculated as the increment rate of the T_1 value in the lesions relative to the non-tumorous liver parenchyma. One-way analysis of variance and Spearman's correlation analysis was used to compare the differences and relationship of T_1 mapping values among the three grades of HCC. A total of 81 lesions were divided into well-differentiated HCC (grades I; n=21), moderately differentiated HCC (grades II; n=40) and poorly differentiated HCC (grades III; n=20) according to the histopathology. The $T_{1(\text{L-H})/H}$ (%) value among grades I, II and III HCC on pre-contrast results and on post-contrast results at the 5-, 10- and 20-min hepatobiliary phase (HBP) were significantly different (P<0.05), and $T_{1(\text{L-H})/H}$ (%) was correlated with the histological grade of HCC at each time point (r=0.637, r=0.554, r=0.499 and r=0.560, respectively, P<0.001). A total of 41 recurrence cases [grade I (n=5), grade II (n=23) and grade III (n=13)] were verified by imaging (CT, MRI or ultrasound) or reoperation. Patients with grade III and grade II HCC had higher recurrence rates compared with that in patients with grade I HCC (P<0.05; median recurrence times were 258 days, 605 days and undefined, respectively). According to the optimal cut-off point for the $T_{1(\text{L-H})/H}$ (%) of the three grades of HCC, patients with HCC in the low $T_{1(\text{L-H})/H}$ (%) value group (≤155.15%) had lower cumulative recurrence rates compared with that in the medium ($T_{1(\text{L-H})/H}$ (%) >155.15% and $T1_{(\text{L-H})/H}$ (%) ≤241.20%) and high ($T_{1(\text{L-H})/H}$ (%) >241.20%) value groups at the 20-min HBP (P<0.05; median recurrence times were undefined, 530 days and 447 days, respectively). These results indicate that the parameters of T_1 mapping would be beneficial for predicting the grading and recurrence of HCC.

Correspondence to: Dr Zhongkui Huang, Department of Radiology, The First Affiliated Hospital of Guangxi Medical University, 22 Shuangyong Road, Nanning, Guangxi 530021, P.R. China
E-mail: huangzhk1205@sina.com; cjr.hzhk@vip.163.com

*Contributed equally

Abbreviations: HCC, hepatocellular carcinoma; Gd-EOB-DTPA, gadolinium-ethoxybenzyl diethylenetriamine pentaacetic acid; MRI, magnetic resonance imaging; HBP, hepatobiliary phase; DWI, diffusion weighted imaging; ROI, region of interest; ROC, receiver operating characteristic

Key words: hepatocellular carcinoma, gadolinium-ethoxybenzyl diethylenetriamine pentaacetic acid, T_1 mapping, Edmondson-Steiner grading, recurrence prediction

Introduction

Primary hepatocellular carcinoma (HCC) is one of the most common malignancies and the third leading cause of cancer-related death worldwide (1). The recurrence rate of HCC 5-years after surgery is >60% in Japan (2). Studies have found that tumor heterogeneity, high degree of differentiation, large size, multicentricity, microvascular invasion, intraoperative extrusion of the tumor, postoperative intervention, macroscopic or microscopic portal venous tumor extension and intrahepatic metastasis were risk factors indicative of poor prognosis after surgery (3-5). Magnetic resonance imaging (MRI) provides valuable imaging information for the preoperative and postoperative evaluation of HCC (6).

Gadolinium-ethoxybenzyl diethylenetriamine pentaacetic (Gd-EOB-DTPA)-enhanced MRI has been widely used in the evaluation of HCC, as it aids in the differential diagnosis, grading and final diagnosis process (7-9). The uptake of Gd-EOB-DTPA in HCC is determined by the expression of

organic anion transporter polypeptide 1B1 (OATP1B1) and OATPIB3, and their activity can predict the signal intensity of Gd-EOB-DTPA-MRI (10). A previous study found that dysplastic nodules (DN) reduced the uptake of Gd-EOB-DTPA and that the enhancement rate of DN in the hepatobiliary phase was higher compared with that in the moderately and poorly differentiated HCC (11). The advantage of Gd-EO-DTPA is that it is taken up by hepatocytes, resulting in the maximal enhancement of normal liver parenchyma in the hepatobiliary phase (HBP) 20 min after injection of the contrast agent (12), thus improving the detection rate of the lesion. A previous study by Zeng *et al* (13) found that Gd-EOB-DTPA-MRI significantly improved the diagnostic and accuracy rates of the liver focal lesions compared with multislice computed tomography and MRI non-specific gadolinium contrast. However, Gd-EOB-DTPA-MRI is inadequate to detect HCC for clinical treatment. Hence, evaluating the liver background and grading of the tumor are crucial factors for a better treatment. A previous study proved that dynamic contrast-enhanced (DCE)-MRI with Gd-EOB-DTPA as a liver-specific MR contrast agent can improve the sensitivity and accuracy in the detection of small HCC (14). In addition, An *et al* (9) reported that the enhanced degree of HCC on the early arterial phase was correlated with its histopathological grade by using multi-parameter quantitative analysis based on Gd-EOB-DTPA-enhanced MRI and diffusion-weighted imaging (DWI). However, the specificity of these multi-parameter methods for grading HCC in the aforementioned studies was not significant. T_1 mapping based on Gd-EOB-DTPA-enhanced MRI has been increasingly used for qualitatively diagnosing diseases of hepatic fibrosis and liver function, and it has achieved good efficiency for discriminating between different degrees of liver fibrosis (15-17). Previous studies found that it was valuable to evaluate T_1 mapping quantitatively at 5-, 10- and 20-min HBP after contrast enhancement for distinguishing interhepatic focal lesions (16,18-20). Previously, retrospective studies demonstrated that T_1 mapping before and after Gd-EOB-DTPA administration can benefit HCC grading, since T_1 mapping could reflect the microscopic changes associated with the tumor to a certain extent (16,18-20).

Up to now, there have been few T_1 mapping studies on HCC grading focusing on the association between T_1 mapping and HCC recurrence (21). The aim of the present study was to investigate the correlation between T_1 mapping and the histopathological grade of HCC, which subsequently provides more preoperative diagnostic information by calculating the T_1 value to predict the recurrence of HCC.

Materials and methods

Patients. Retrospective data collection and analysis was approved by the Institutional Review Board of The First Affiliated Hospital of Guangxi Medical University (Nanning, China). A total of 75 consecutive patients who were diagnosed with primary HCC, confirmed by histopathological examination, between September 2015 and March 2017, were enrolled for the present study. All patients underwent a hepatectomy within 2 weeks of Gd-EOB-DTPA-enhanced MRI. Inclusion criteria were as follows: i) Patients who underwent Gd-EOB-DTPA-enhanced MRI before hepatectomy or liver biopsy; ii) patients who underwent surgical resection treatment; and iii) patients who were confirmed to have primary HCC by histopathological staining. Exclusion criteria were as follows: i) Tumor size >1 cm; ii) previous interventional treatment; iii) metastasis; and iv) diffuse-type HCC. Recurrence was defined as a new lesion that was observed by two experienced radiologists on imaging (CT, MRI and ultrasound) or confirmed by pathology after rehepatectomy. All the patients were followed up until September 30, 2018, or until mortality. For patients who were unable to undergo reexamination in person at The First Affiliated Hospital of Guangxi Medical University, follow-up was performed 3 months after surgery, via telephone. Written informed consent was obtained from all patients with HCC. For the histopathological examination, the HCC tissues and corresponding non-cancerous were fixed in 4% neutral formaldehyde at 65˚C for 2 h and subsequently the paraffin-embedded tissues were cut into 4 μm sections. Following which hematoxylin and eosin staining was performed for 1 h at room temperature. Pathological sections were observed under an Olympus BX53 light microscope (magnification, x100 and x200) and the features of HCC were observed as follows: The hepatocytes were polygonal or round, and arranged as nests or cables; the nuclei were enlarged and its nucleolus was deeply stained and there was an abundance of blood sinuses in the cancer nests.

MRI protocols. All MR scans were conducted on a 3T MRI scanner (Magnetom Verio; Siemens Healthineers) with an 8-channel phased-array body coil. Half-fourier acquisition single-shot turbo spin echo sequence, axial turbo spin echo T2-weighted free breathing with fat suppression sequence, and breath-hold axial single-shot echo planar imaging DWI fat-suppressed sequence were performed prior to contrast enhancement. An axial T_1-weighted three-dimensional spoiled gradient echo volume interpolated body examination fat-suppressed sequence was performed to acquire DCE-MRI data. A bolus of 0.025 mmol/kg Gd-EOB-DTPA (Bayer AG) was injected at a rate of 2 ml/sec through the cubital vein, followed by a 20-ml saline flush at the same rate. T_1 mapping was performed before and at the 5, 10 and 20 min delay phases after Gd-EOB-DTPA administration. The sequence parameters used are listed in Table I.

T_1 value measurement. All MRI data obtained from the patients were analyzed to measure T_1 relaxation time using operator-defined regions of interest (ROI). The ROI with an area of 1-1.2 cm^2 was drawn manually on the lesion and non-tumorous liver parenchyma (1-2 cm distant from the margin of the tumor) by two experienced radiologists, respectively, who were blinded to the histopathological information, and each ROI was taken three times to measure the mean T_1 values for further analysis. In case of conflicts, the decision was negotiated. All measurements were performed to avoid bile duct, hemorrhage, necrosis, cystic, fat, blood vessels and bile ducts, artifacts, selecting the maximum tumor cross-sectional area (Fig. 1). Subsequently, the average values were calculated and the T_1 value was expressed as the mean ± standard deviation (SD). The increasing rate of T_1 value in the HCC lesion [$T1_{(L\text{-}H)/H}$ (%)] was calculated using the following equation: $T_{1(L\text{-}H)/H}$ (%)=(T_{1L}-T_{1H})/T_{1H} x100, where L indicates the lesion and H indicates the hepatic parenchyma.

Table I. Magnetic resonance imaging sequences used in the present study.

Sequences	Repetition time, msec	Echo time, msec	Flip angle, °	Slice thickness, mm	Matrix	Field of view, mm
Plain scan						
T1WI, tra	3.96	1.41	9	4.5	224x320	350x350
In/outphase	171	2.31	70	6	192x256	380x380
T2WI, tra	2,930	89	133	6	240x320	400x400
T2WI, cro	1,800	95	160	6	224x320	380x380
VIBE-T1 mapping	3.96	1.41	2/15	4.5	224x320	350x350
DWI	9,200	66		6	118x148	420x420
Dynamic contrast-enhanced						
T1WI, tra	4.56	1.48	30	4.5	224x320	350x350
T1WI, cor	3.32	1.17	9	4	216x288	350x350
VIBE-T1 mapping	3.96	1.41	2/15	4.5	224x320	350x350

T1WI, T1-weighted imaging; T2WI, T2-weighted imaging; DWI, diffusion-weighted imaging; DCE, dynamic contrast-enhanced; VIBE, volumetric interpolated breath-hold examination; tra, transversal; cor, coronal.

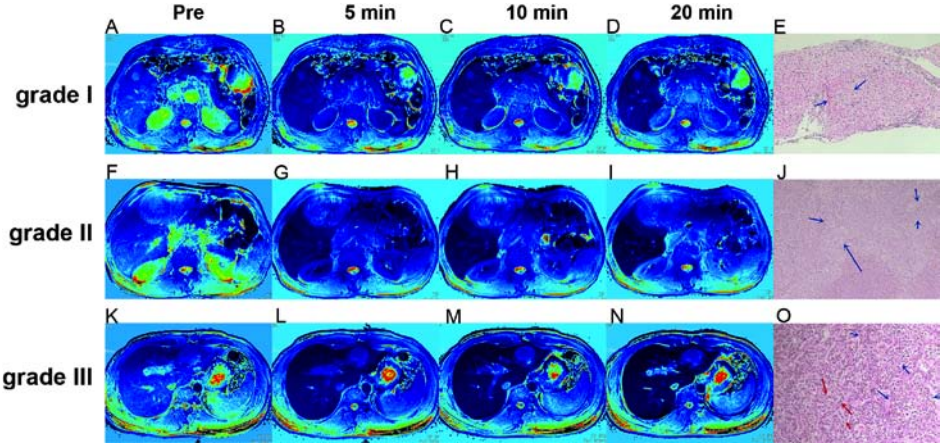

Figure 1. Regions of interest in tumor and non-tumor liver parenchyma at different time points after HBP enhancement in 3 representative patients with Edmondson-Steiner grade I, II and III HCC. (A-D) T_1 mapping of a 78-year old male patient with HCC grade I at (A) pre-contrast and at (B) 5, (C) 10 and (D) 20 min after administration of Gd-EOB-DTPA, respectively. (F-I) T_1 mapping of a 62-year old male patient with HCC grade II at (F) pre-contrast and at (G) 5, (H) 10 and (I) 20 min after administration of Gd-EOB-DTPA, respectively. (K-N) T_1 mapping of a 30-year old male patient with HCC grade III at (K) pre-contrast and at (L) 5, (M) 10 and (N) 20 min after administration of Gd-EOB-DTPA, respectively. (E, J and O) Hematoxylin and eosin staining images of grades I, II and III of HCC. (E) Grade I HCC at x100 magnification. The tumor cells are arranged into irregular thick lines, which are more than three layers, indicated by the blue arrows. (J) Grade II HCC at x200 magnification. The tumor cells are arranged in a disorderly manner with less atypia, as indicated by the blue arrows. (O) Grade III HCC at x100 magnification, The lines of cancer cells were markedly thickened, as indicated by the blue arrows, and the atypical cancer cells showed enlarged nuclei with deeply stained nucleoli, as indicated by the red arrows. Pre, pre-contrast; HHC, hepatocellular carcinoma; Gd-EOB-DTPA, gadolinium-ethoxybenzyl diethylenetriamine pentaacetic acid.

The $T_{1(L\text{-}H)/H}$ (%) values before and at the 5-, 10- and 20-min HBP after Gd-EOB-DTPA administration for each patient were respectively calculated by the aforementioned equation.

Statistical analysis. Analyses were performed using SPSS software (version 22.0; IBM Corp.). Statistical charts were created using GraphPad Prism v5.01 (Graphpad Software, Inc.). Descriptive statistics (mean ± SD), such as mean diameter were provided when no quantifiable data was available. One-way analysis of variance with the least significant difference test were used to compare the differences in the increment rate of the T_1 value in the lesions relative to non-tumorous liver parenchyma [$T1_{(L\text{-}H)/H}$ (%)] among different grades of HCC. Spearman's correlation analysis was used to evaluate the correlation between the increasing rate of T_1 values and HCC grading. Patients who were lost to follow-up or died (due to an accident unrelated to HCC or from postoperative complications) during the follow-up period were censored. Receiver operating characteristic (ROC) curve analyses were conducted for $T_{1(L\text{-}H)/H}$ (%) of grade I, II and III HCC. The cut-off values of $T_{1(L\text{-}H)/H}$ (%) between grades I and II, grades II and III HCC were obtained, respectively; and then the cumulative recurrence rates of the three groups rearranged by these two cut-off values of $T1_{(L\text{-}H)/H}$ (%) were also evaluated using Kaplan-Meier method and log-rank test. $P<0.05$ was considered to indicate a statistically significant difference.

Results

Patient characteristics. A total of 75 patients (66 men and 9 women; mean age, 52.89 years; age range, 23-79 years) with 81 lesions were included in the present study. According to the Liver Disease Symposium on Barcelona Clinic Liver Cancer (BCLC) staging system for hepatocellular carcinoma (22), the HCC cases were classified as BCLC stage A, B, C and D. A total of 81 lesions with a mean diameter of 4.13±0.32 cm (range 1.2-15 cm) were measured. Pathological diagnosis and grading were made according to the Edmondson-Steiner grading system (23). Due to research population restrictions, Edmondson-Steiner grade IV of HCC was not included in the present study. In our study, 19 patients with 21 lesions (25.93%) were classified as grade I, 37 patients with 40 lesions (49.38%) as grade II and 19 patients with 20 lesions (24.69%) as grade III. Recurrence of HCC was observed in 41 (54.67%) out of 75 patients during the follow-up period (median, 639.00 days; range, 42.00-973.00 days), and 1 patient was lost to follow-up after 490 days from the last reexamination. A total of 3 patients (2 HCC grade II and 1 HCC grade III) died 369, 195 and 398 days, respectively, after hepatectomy. The 41 recurrence cases [grade I (n=5), grade II (n=23), and grade III (n=13)] were verified by imaging (CT, MRI and ultrasound) or reoperation. The baseline characteristics of the patients are shown in Table II.

Comparison of T_1 mapping of different grades of HCC at different time points. On pre-contrast, $T_{1(L\text{-}H)/H}$ (%) values for grade I, II and III HCC were 31.42±15.77, 56.07±21.42 and 78.21±27.68, respectively; at 5 min after enhancement, $T_{1(L\text{-}H)/H}$ (%) values were 85.48±73.06, 132.63±37.27 and 172.82±71.48, respectively; at 10 min after enhancement, $T1_{(L\text{-}H)/H}$ (%) values were 115.43±82.25, 190.81±66.58 and 226.13±101.49, respectively; and at 20 min after enhancement, $T1_{(L\text{-}H)/H}$ (%) values were 149.46±97.32, 247.59±85.16 and 333.95±134.99, respectively. $T_{1(L\text{-}H)/H}$ (%) was moderately correlated with Edmondson-Steiner HCC grading both at pre-contrast, and at 5, 10 and 20 min after administration of Gd-EOB-DTPA, respectively (r=0.637, r=0.554, r=0.499 and r=0.560, respectively; P<0.001). On pre-contrast and on post-contrast at the 5- and 20-min HBP, multiple comparisons of $T_{1(L\text{-}H)/H}$ (%) in the three groups of HCC were significantly different (P<0.05). On post-contrast at 10 min, the differences in $T_{1(L\text{-}H)/H}$ (%) value between grades I and II, and grades I and III were statistically significant (P<0.05), while $T1_{(L\text{-}H)/H}$ (%) values between grades II and III showed no significant differences (P>0.05). The $T_{1(L\text{-}H)/H}$ (%) value markedly increased for each grade of HCC at each time point and the $T1_{(L\text{-}H)/H}$ (%) of different HCC grades increased after enhancement compared with pre-enhancement (Fig. 2).

Variation of $T_{1(L\text{-}H)/H}$ (%) and the T_1 relaxation time at each time point. The variation trend of $T_{1(L\text{-}H)/H}$ (%) and the T_1 relaxation time in HCC lesions and non-tumorous liver parenchyma of differentiation grades at each time point are shown in Fig. 3. The value of $T_{1(L\text{-}H)/H}$ (%) after enhancement was higher compared with that pre-contrast, and $T1_{(L\text{-}H)/H}$ (%) was significantly increased with increasing delay time after contrast medium administration, with the most significant difference observed at the 20-min HBP (P<0.05). For HCC lesions, the T_1 value was lowest at 5 min, but increased gradually from 10 to 20 min, with overlapping results for grades II and III. For liver parenchyma, the higher the malignancy degree of HCC

Table II. Clinical characteristics of the 75 patients with primary hepatocellular carcinoma.

Characteristic	Value
Age, years[a]	52.89±1.38
Sex, n (%)	
Male	66 (88.00)
Female	9 (12.00)
Mean size, cm[a]	4.13±0.32
Underlying disease, n (%)	
HBV	66 (88.00)
HCV	8 (10.67)
HBV + HCV	8 (10.67)
Clonorchis	9 (12.00)
Cirrhosis	44 (58.67)
Child-Pugh classification[b], n (%)	
A	70 (93.33)
B	5 (6.67)
BCLC stage, n (%)	
A	52 (69.33)
B	17 (22.67)
C	6 (8.00)
D	0 (0.00)
AFP, n (%)	
Normal <20 ng/ml	27 (36.00)
Abnormal ≥20 ng/ml	48 (64.00)

[a]Mean ± standard deviation; [b](33). HBV, hepatitis B virus; HCV, hepatitis B virus; BCLC, Barcelona Clinic Liver Cancer; AFP, α-fetoprotein.

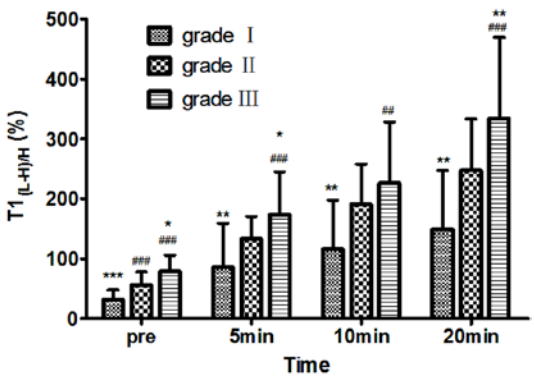

Figure 2. One-way analysis of variance was used to analyze the differences in $T_{1(L\text{-}H)/H}$ (%) value in the 81 HCC lesions between different Edmondson-Steiner grades at pre-contrast, and 5, 10 and 20 min after administration of gadolinium-ethoxybenzyl diethylenetriamine pentaacetic acid, respectively. ##P<0.01 and ###P<0.001 vs. grade I; *P<0.05, **P<0.01 and ***P<0.001 vs. grade II. Pre, pre-contrast; L, lesion; H, hepatic parenchyma; HHC, hepatocellular carcinoma.

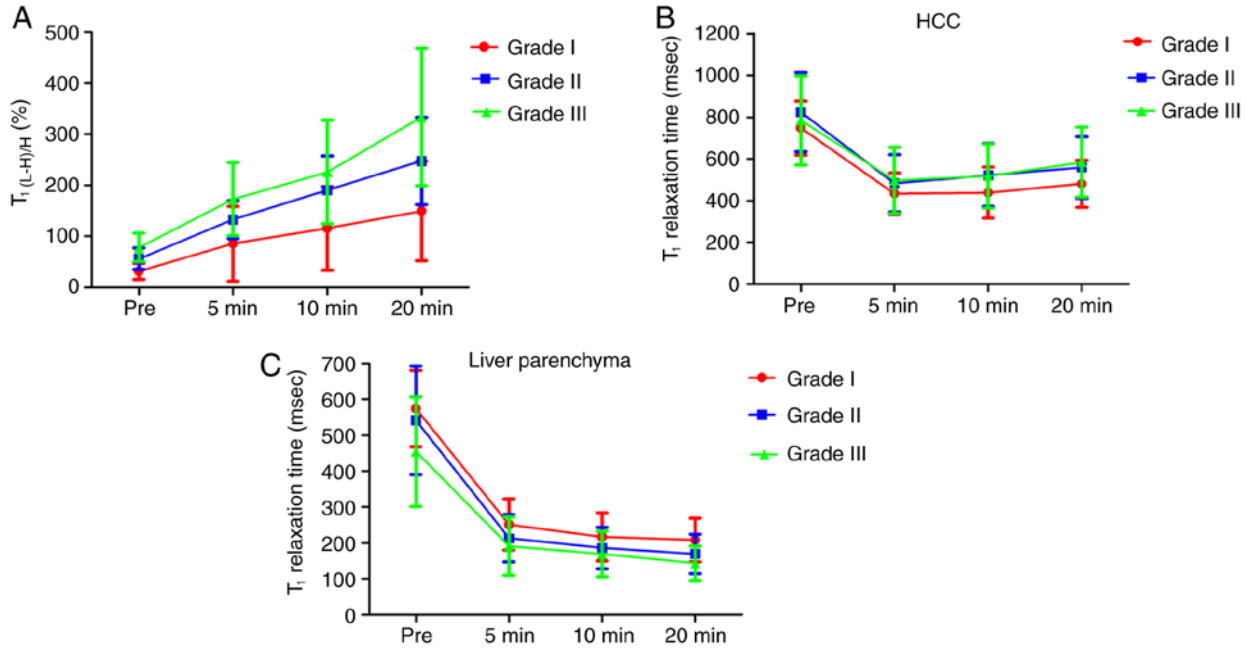

Figure 3. Variation trend of $T_{1(L-H)/H}$ (%), and T_1 relaxation time in HCC lesion and non-tumorous liver parenchyma of various differentiation grades at each time point. (A) $T_{1(L-H)/H}$ (%) was increased with increasing time after administration, and the most significant difference was observed at 20 min in the HBP ($P<0.05$). (B) T_1 value of HCC was lowest at 5 min, but increased gradually from 10 to 20 min, with overlapping results for grades II and grade III. (C) T_1 value of liver parenchyma declined rapidly from 5 to 10 min, and declined slowly from 10 to 20 min for grade I HCC, while that of grades II and III HCC declined slowly from 5 to 20 min HBP. This linear trend showed that the higher the grade of HCC, the shorter the T_1 relaxation time of liver parenchyma and showed no statistically significant differences ($P>0.05$). HHC, hepatocellular carcinoma.

the lower the T_1 value, particularly in the pre-contrast imaging. The T_1 value of liver parenchyma decreased quickly from pre-contrast to 10 min post-enhancement, and then slowly from the 10- to 20-min HBP, for the three grades of HCC. However, the T_1 value of non-tumorous liver parenchyma at each time point showed no statistical differences among the different grades of HCC ($P>0.05$).

Survival analysis for 3 groups of patients with HCC. At the 20-min HBP, the optimal cut-off point for the $T1_{(L-H)/H}$ (%) of grade I and II, II and III HCC based on the ROC curve analysis were 155.15 and 241.20%, respectively (Fig. 4). The patients were subsequently classified into a low group ($T_{1(L-H)/H}$ (%) ≤155.15%), a medium group ($T_{1(L-H)/H}$ (%) >155.15% and $T_{1(L-H)/H}$ (%) ≤ 241.20%) and a high group ($T_{1(L-H)/H}$ (%) >241.20%). During the follow-up period, 41 out of 75 patients developed recurrence; 5 cases (5/19) were Edmondson-Steiner grade I, 23 cases (23/37) were grade II and 13 cases (13/19) were grade III HCC, and their median recurrence times were undefined, 605 days and 258 days, respectively. The recurrence rates of patients with grade II and grade III HCC were significantly higher compared with that of patients with grade I HCC ($P<0.05$) (Fig. 5). The median recurrence time of the low $T_{1(L-H)/H}$ (%) value group (n=17), the medium group (n=22) and the high group (n=37) were undefined, 530 days and 447 days, respectively. Recurrence rates also increased with increasing $T_{1(L-H)/H}$ (%) from the low group to the medium and from the low to the high groups in the 20-min HBP ($P<0.05$). The patients with HCC classified with low $T1_{(L-H)/H}$ (%) values had lower cumulative recurrence rates compared with that in patients classified as medium and high value groups ($P=0.028$ and $P=0.001$, respectively). The cumulative recurrence rates of the patients with medium $T1_{(L-H)/H}$ (%) values were lower compared with that of the high value group, but the results were not significantly different ($P>0.05$) (Fig. 6).

Discussion

In the present study, Gd-EOB-DTPA-enhanced T_1 mapping was used to quantitatively evaluate HCC. The results demonstrated that $T_{1(L-H)/H}$ (%) was positively correlated with the Edmondson-Steiner grade of HCC. Gd-EOB-DTPA-enhanced T_1 relaxation time-based parameter performed accurate diagnostic grading of HCC. Gd-EOB-DTPA has a T_1 shortening effect and highlights the lesions in the liver. T_1 relaxation time is an objective quantitative parameter. The T_1 relaxation time was measured on the basis of the MR relaxation technique and is directly correlated with the concentration of Gd-EOB-DTPA (24). In the present study, the majority of patients with HCC had a history of chronic liver disease. The increment rate of the T_1 value, which increased in the lesions relative to the non-tumorous liver parenchyma [$T_{1(L-H)/H}$ (%)], reflects the true T_1 relaxation time of the lesion. $T_{1(L-H)/H}$ (%) was positively correlated with the Edmondson-Steiner grade of HCC. Due to the higher grade of HCC, the differences in liver function between tumor and normal liver parenchyma were more visible and the differences in the concentration of the Gd-EOB-DTPA in the tissue were markedly visible in the three grades of HCC at 5 min, 10 min and 20 min HBP after enhancement, respectively, leading to a higher rate-of-change of T_1 values in the lesions when compared with that in non-tumorous liver parenchyma. Kogita *et al* (11) also confirmed that the concentration of Gd-EOB-DTPA uptake in HCC was positively associated with the degree of HCC differentiation. Moreover,

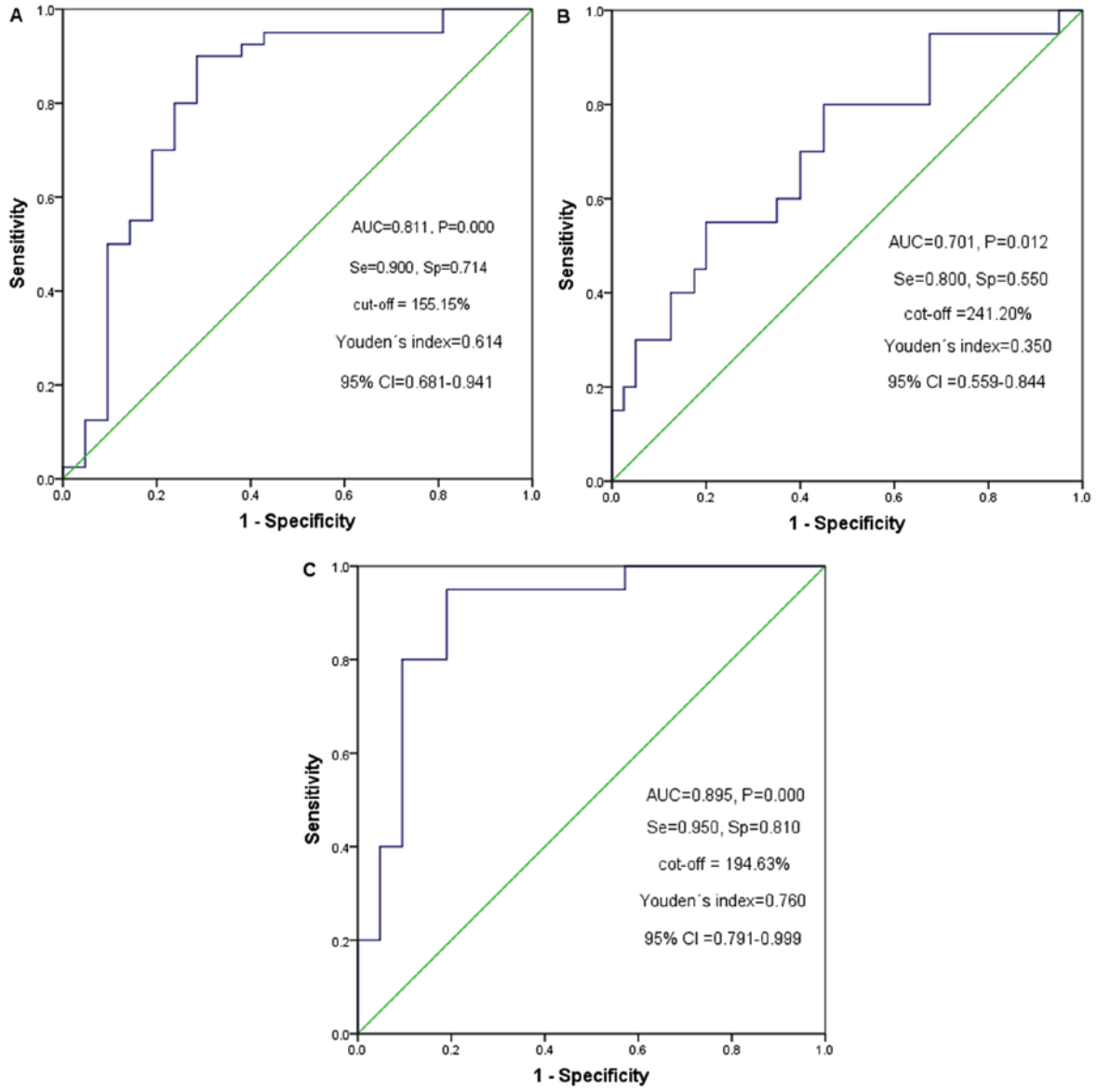

Figure 4. ROC curve of the optimal cut-off point for the $T_{1(L\text{-}H)/H}$ (%) of grades I, II and III HCC. ROC curve of (A) grade I and II HCC, (B) grade II and III HCC, and (C) grade I and III HCC. ROC, receiver operating characteristic; AUC, area under the curve; Se, sensitivity; Sp, specificity; CI, confidence interval; HHC, hepatocellular carcinoma.

the $T1_{(L\text{-}H)/H}$ (%) was highest at the 20 min HBP in the present study, as the concentration of Gd-EOB-DTPA reached a peak value at 20 min after enhancement, while the concentration of the contrast agent in HCC cells remained lower.

In the present study, the T_1 value of the non-tumorous liver parenchyma, especially on pre-contrast, was lower with a higher malignant degree of HCC ($P<0.05$) and reached a peak at 20 min, which was similar to the result found in a previous study (11). The T_1 value of grade I HCC was lowest at 5 min, and increased gradually at 10 and 20 min, with partly overlapping values in grade II and grade III HCC; however, the $T_{1(L\text{-}H)/H}$ (%) of the three grades of HCC showed significant differences at pre-contrast, 5 min, and 20 min HBP, respectively. This result might be due to the liver background affecting the T_1 value of the tumor. These results suggest that higher grades of HCC will uptake smaller amounts of Gd-EOB-DTPA, and that the absorption rate of the contrast agent is significantly different between HCC and non-tumorous liver parenchyma at different time points. This may be due to the absence of normal liver function for patients with HCC and due to the fact that Gd-EOB-DTPA is mainly observed in the extracellular space and intravascular area at the beginning of enhancement. Furthermore, the HCC cells uptake the contrast agents slowly, resulting in less uptake of the contrast agents into the cells, and the concentration of Gd-EOB-DTPA in the intracellular area increases gradually post-contrast. By contrast, the non-tumorous liver parenchyma uptakes Gd-EOB-DTPA faster than HCC, leading to two types of T_1 value-time curves (Fig. 3B and C).

With a higher degree of malignancy, new blood vessels are formed, which are more likely to invade the surrounding liver parenchyma, leading to recurrence (25). Previous studies have reported that HCC recurrence is related to heterogeneity, multicentric type and expression of vascular endothelial growth factor of the tumor (26,27). In the present study, the patients with a higher grade of HCC had a higher

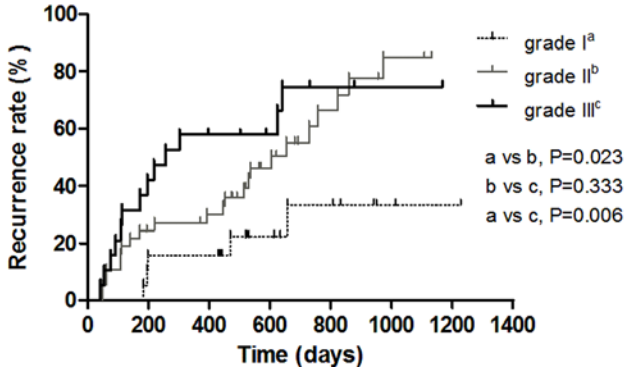

Figure 5. Recurrence curve of three grades of HCC after surgery. Recurrence rates of grades II and III HCC were significantly higher compared with that of grade I HCC (P=0.023 and P=0.006, respectively). Patients with grade III HCC had higher recurrence rates compared with patients with grade II HCC, at 800 days after resection, but the differences were not significantly different (P>0.05). HHC, hepatocellular carcinoma.

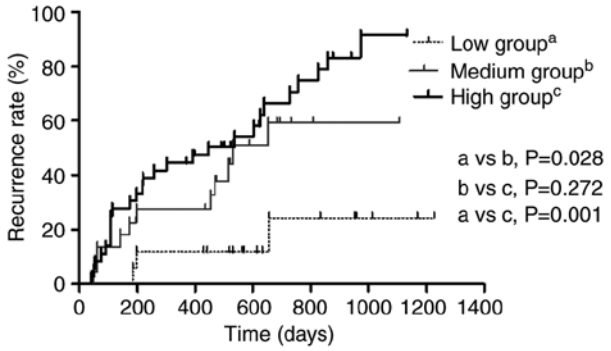

Figure 6. Kaplan-Meier analysis and log-rank test was performed for the 3 groups classified according to the two cut-off $T_{1(L\text{-}H)/H}$ (%) values of grades I and II, II and III HCC, 155.15 and 241.20%, respectively, at 20 min HBP. Recurrence curve showed the recurrence rates of HCC with low, medium and high $T_{1(L\text{-}H)/H}$ (%) values following surgery.

recurrence rate. Patients with grade I HCC had the lowest cumulative recurrence rates compared with patients with grade II and III HCC. Patients with grade III HCC had a higher but indistinctive recurrence rate compared with that in patients with grade II HCC, which was ~800 days after resection. We hypothesized that the absence of a significant difference may be due to the small sample size for grade III HCC compared with that of grade II HCC, therefore, studies with a larger sample size are required in the future. This may also be due to tumorous microvascular invasion and the histological grade of the cirrhosis (28). It is possible that the recurrent tumor may invade the surrounding liver parenchyma, promote cellular density and increase the formation of new vessels. If the tumor invades the microvasculature of the surrounding liver parenchyma and local liver function is damaged, the excretion of Gd-EOB-DTPA can be blocked (29,30). In addition, Zhou *et al* (4) reported that the Edmondson-Steiner grade of HCC was an independent risk factor for recurrence after resection. Mori *et al* (31) also demonstrated that poorly differentiated HCC was more likely to have intrahepatic metastasis and recurrence compared with well-/moderately differentiated HCC. The results from the present study revealed that the HCC patients with lower $T_{1(L\text{-}H)/H}$ (%) values had lower cumulative recurrence rates compared with those patients with higher $T_{1(L\text{-}H)/H}$ (%) values at the 20-min HBP. Shen *et al* (32) also recently found that a poorly differentiated tumor had a negative impact on the recurrence and long-term survival of patients with solitary HBV-associated HCCs after curative hepatectomy. This suggests that the lower the differentiation of HCC is, the more likely it is to recur, which was partly consistent with the study by Shen *et al* (32). Hence, if Gd-EOB-DTPA-enhanced MRI could be used to detect small lesions with high sensitivity, and grade HCC with Gd-EOB-DTPA-MRI T_1 mapping before surgery, it will contribute to a more appropriate therapy for patients with HCC. Precise preoperative information regarding the characterization, prognosis and staging of HCC is essential.

However, the present study has several limitations. Firstly, the sample size is small, particularly for well- and poorly differentiated HCC. A further study with a larger sample size and longer follow-up time is required. Secondly, due to the small number of recurrent HCC patients, the effect of liver function, liver fibrosis and other liver backgrounds on the recurrence of HCC were not analyzed.

In conclusion, the parameters of T_1 mapping, $T_{1(L\text{-}H)/H}$ (%) are positively correlated with the degree of malignancy of HCC. Higher grade HCC has a higher recurrence rate. The recurrence rate of HCC patients with high $T_{1(L\text{-}H)/H}$ (%) was consistently significantly higher compared with that of patients with low $T_{1(L\text{-}H)/H}$ (%). Although a larger-scale prospective study is required to confirm these findings, the results showed that T_1 mapping on Gd-EOB-DTPA-enhanced MRI was beneficial in HCC applications and provided valuable information for HCC grading and recurrence prediction.

Acknowledgements

Not applicable.

Funding

The present study was funded by the National Natural Science Foundation of China (grant no. 81260214).

Availability of data and materials

All data generated or analyzed during this study are included in this published article.

Authors' contributions

TFY conceived the study design and drafted the manuscript. ZKH provided the concept of the study and reviewed the manuscript. YJG collected the samples and researched the literature. XLQ was involved in data acquisition, statistical analysis, manuscript preparation and editing. ZPZ participated in the data analysis. WML, MZW and XYZ interpreted the data and revised the manuscript. LLL made substantial contributions to conception and design and guaranteed that any questions related to the accuracy or integrity of any part of the work were appropriately investigated and resolved. All the authors have read and approved the final manuscript.

Ethics approval and consent to participate

Retrospective data and tissue collection and analysis were approved by the Institutional Review Board of The First Affiliated Hospital of Guangxi Medical University (approval no. 2012-KY-223).

Patient consent for publication

Not applicable.

Competing interests

The authors declare that they have no competing interests.

References

1. Hu Y, Wu J, Li S and Zhao X: Correlation between CT features and liver function and p53 expression in hepatitis, cirrhosis and hepatocellular carcinoma. Oncol Lett 16: 4297-4302, 2018.
2. Imamura H, Matsuyama Y, Tanaka E, Ohkubo T, Hasegawa K, Miyagawa S, Sugawara Y, Minagawa M, Takayama T, Kawasaki S and Makuuchi M: Risk factors contributing to early and late phase intrahepatic recurrence of hepatocellular carcinoma after hepatectomy. J Hepatol 38: 200-207, 2003.
3. Ariizumi S, Kitagawa K, Kotera Y, Takahashi Y, Katagiri S, Kuwatsuru R and Yamamoto M: A non-smooth tumor margin in the hepatobiliary phase of gadoxetic acid disodium (Gd-EOB-DTPA)-enhanced magnetic resonance imaging predicts microscopic portal vein invasion, intrahepatic metastasis, and early recurrence after hepatectomy in patients with hepatocellular carcinoma. J Hepatobiliary Pancreat Sci 18: 575-585, 2011.
4. Zhou L, Rui JA, Zhou WX, Wang SB, Chen SG and Qu Q: Edmondson-Steiner grade: A crucial predictor of recurrence and survival in hepatocellular carcinoma without microvascular invasio. Pathol Res Pract 213: 824-830, 2017.
5. Nathan H, Schulick RD, Choti MA and Pawlik TM: Predictors of survival after resection of early hepatocellular carcinoma. Ann Surg 249: 799-805, 2009.
6. Kim JH, Min YW, Gwak GY, Paik YH, Choi MS, Lee JH, Koh KC and Paik SW: The utility of gadoxetic acid-enhanced magnetic resonance imaging in the surveillance for postoperative recurrence of hepatocellular carcinoma. Medicine (Baltimore) 95: e5666, 2016.
7. Peng Z, Jiang M, Cai H, Chan T, Dong Z, Luo Y, Li ZP and Feng ST: Gd-EOB-DTPA-enhanced magnetic resonance imaging combined with T1 mapping predicts the degree of differentiation in hepatocellular carcinoma. BMC Cancer 16: 625, 2016.
8. Chang WC, Chen RC, Chou CT, Lin CY, Yu CY, Liu CH, Chou JM, Hsu HH and Huang GS: Histological grade of hepatocellular carcinoma correlates with arterial enhancement on gadoxetic acid-enhanced and diffusion-weighted MR images. Abdom Imaging 39: 1202-1212, 2014.
9. An C, Park MS, Jeon HM, Kim YE, Chung WS, Chung YE, Kim MJ and Kim KW: Prediction of the histopathological grade of hepatocellular carcinoma using qualitative diffusion-weighted, dynamic, and hepatobiliary phase MRI. Eur Radiol 22: 1701-1708, 2012.
10. Nassif A, Jia J, Keiser M, Oswald S, Modess C, Nagel S, Weitschies W, Hosten N, Siegmund W and Kuhn JP: Visualization of hepatic uptake transporter function in healthy subjects by using gadoxetic acid-enhanced MR imaging. Radiology 264: 741-750, 2012.
11. Kogita S, Imai Y, Okada M, Kim T, Onishi H, Takamura M, Fukuda K, Igura T, Sawai Y, Morimoto O, *et al*: Gd-EOB-DTPA-enhanced magnetic resonance images of hepatocellular carcinoma: Correlation with histological grading and portal blood flow. Eur Radiol 20: 2405-2413, 2010.
12. Lee SA, Lee CH, Jung WY, Lee J, Choi JW, Kim KA and Park CM: Paradoxical high signal intensity of hepatocellular carcinoma in the hepatobiliary phase of Gd-EOB-DTPA enhanced MRI: Initial experience. Magn Reson Imaging 29: 83-90, 2011.
13. Zeng MS, Ye HY, Guo L, Peng WJ, Lu JP, Teng GJ, Huan Y, Li P, Xu JR, Liang CH and Breuer J: Gd-EOB-DTPA-enhanced magnetic resonance imaging for focal liver lesions in Chinese patients: A multicenter, open-label, phase III study. Hepatobiliary Pancreat Dis Int 12: 607-616, 2013.
14. Park JH, Kang JH, Lee YJ, Kim KI, Lee TS, Kim KM, Park JA, Ko YO, Yu DY, Nahm SS, *et al*: Evaluation of diethylnitrosamine- or hepatitis B virus X gene-induced hepatocellular carcinoma with 18F-FDG PET/CT: A preclinical study. Oncol Rep 33: 347-353, 2015.
15. Haimerl M, Verloh N, Zeman F, Fellner C, Muller-Wille R, Schreyer AG, Stroszczynski C and Wiggermann P: Assessment of clinical signs of liver cirrhosis using T1 mapping on Gd-EOB-DTPA-enhanced 3T MRI. PLoS One 8: e85658, 2013.
16. Zhou ZP, Long LL, Qiu WJ, Cheng G, Huang LJ, Yang TF and Huang ZK: Comparison of 10- and 20-min hepatobiliary phase images on Gd-EOB-DTPA-enhanced MRI T1 mapping for liver function assessment in clinic. Abdom Radiol (NY) 42: 2272-2278, 2017.
17. Ding Y, Rao SX, Zhu T, Chen CZ, Li RC and Zeng MS: Liver fibrosis staging using T1 mapping on gadoxetic acid-enhanced MRI compared with DW imaging. Clin Radiol 70: 1096-1103, 2015.
18. Yoshimura N, Saito K, Saguchi T, Funatsu T, Araki Y, Akata S and Tokuuye K: Distinguishing hepatic hemangiomas from metastatic tumors using T1 mapping on gadoxetic-acid-enhanced MRI. Magn Reson Imaging 31: 23-27, 2013.
19. Zhou ZP, Long LL, Qiu WJ, Cheng G, Huang LJ, Yang TF and Huang ZK: Evaluating segmental liver function using T1 mapping on Gd-EOB-DTPA-enhanced MRI with a 3.0 Tesla. BMC Med Imaging 17: 20, 2017.
20. Peng Z, Li C, Chan T, Cai H, Luo Y, Dong Z, Li ZP and Feng ST: Quantitative evaluation of Gd-EOB-DTPA uptake in focal liver lesions by using T1 mapping: Differences between hepatocellular carcinoma, hepatic focal nodular hyperplasia and cavernous hemangioma. Oncotarget 8: 65435-65444, 2017.
21. Wang WT, Zhu S, Ding Y, Yang L, Chen CZ, Ye QH, Ji Y, Zeng MS and Rao SX: T1 mapping on gadoxetic acid-enhanced MR imaging predicts recurrence of hepatocellular carcinoma after hepatectomy. Eur J Radiol 103: 25-31, 2018.
22. Llovet JM, Fuster J and Bruix J: Prognosis of hepatocellular carcinoma. Hepatogastroenterology 49: 7-11, 2002.
23. Edmondson HA and Steiner PE: Primary carcinoma of the liver: A study of 100 cases among 48,900 necropsies. Cancer 7: 462-503, 1954.
24. Bae KE, Kim SY, Lee SS, Kim KW, Won HJ, Shin YM, Kim PN and Lee MG: Assessment of hepatic function with Gd-EOB-DTPA-enhanced hepatic MRI. Dig Dis 30: 617-622, 2012.
25. Zhang W, Tan Y, Jiang L, Yan L, Li B, Wen T and Yang J: Liver resection associated with better outcomes for single large hepatocellular carcinoma located in the same section. Medicine (Baltimore) 96: e6246, 2017.
26. Liu K, Hao M, Ouyang Y, Zheng J and Chen D: CD133(+) cancer stem cells promoted by VEGF accelerate the recurrence of hepatocellular carcinoma. Sci Rep 7: 41499, 2017.
27. Barreto SG, Brooke-Smith M, Dolan P, Wilson TG, Padbury RT and Chen JW: Cirrhosis and microvascular invasion predict outcomes in hepatocellular carcinoma. ANZ J Surg 83: 331-335, 2013.
28. Park YK, Kim BW, Wang HJ and Kim MW: Hepatic resection for hepatocellular carcinoma meeting Milan criteria in Child-Turcotte-Pugh class a patients with cirrhosis. Transplant Proc 41: 1691-1697, 2009.
29. Tsuda N, and Matsui O: Cirrhotic rat liver: Reference to transporter activity and morphologic changes in bile canaliculi-gadoxetic acid-enhanced MR imaging. Radiology 256: 767-773, 2010.
30. Norén B, Dahlström N, Forsgren MF, Dahlqvist Leinhard O, Kechagias S, Almer S, Wirell S and Smedby Ö and Lundberg P: Visual assessment of biliary excretion of Gd-EOB-DTPA in patients with suspected diffuse liver disease-A biopsy-verified prospective study. Eur J Radiol Open 2: 19-25, 2015.
31. Mori Y, Tamai H, Shingaki N, Hayami S, Ueno M, Maeda Y, Moribata K, Deguchi H, Niwa T, Inoue I, *et al*: Hypointense hepatocellular carcinomas on apparent diffusion coefficient mapping: Pathological features and metastatic recurrence after hepatectomy. Hepatol Res 46: 634-641, 2016.
32. Shen J, Liu J, Li C, Wen T, Yan L and Yang J: The impact of tumor differentiation on the prognosis of HBV-associated solitary hepatocellular carcinoma following hepatectomy: A propensity score matching analysis. Dig Dis Sci 63: 1962-1969, 2018.
33. Kok B and Abraldes JG: Child-pugh classification: Time to abandon? Semin Liver Dis 39: 96-103, 2019.